Continuous Precipitation Polymerization of Vinylidene Fluoride in Supercritical Carbon Dioxide: Formation of Polymers with Bimodal Molecular Weight Distributions

Manish K. Saraf,[†] Sylvain Gerard,[†] Louis M. Wojcinski II,[†] Paul A. Charpentier,[†,§] Joseph M. DeSimone,*[,†,‡] and George W. Roberts*[,†]

Department of Chemical Engineering, North Carolina State University, Box #7905, Raleigh, North Carolina 27695-7905, and Department of Chemistry, University of North Carolina-Chapel Hill, Venable and Kenan Laboratories, CB#3290, Chapel Hill, North Carolina 27599

Received March 8, 2002; Revised Manuscript Received July 10, 2002

ABSTRACT: The polymerization of vinylidene fluoride in supercritical carbon dioxide was studied in a continuous stirred tank reactor using diethylperoxydicarbonate as the free radical initiator. Experiments were carried out to investigate the effect of inlet monomer concentration, temperature, average residence time, and agitation on the polymerization rate, the average molecular weights, and the molecular weight distribution of the poly(vinylidene fluoride). A homogeneous kinetic model that includes inhibition due to chain transfer to monomer predicted the polymerization rates reasonably well. However, imperfect mixing, rather than a chemical effect, may have caused the apparent inhibition observed at high monomer concentrations. At inlet monomer concentrations greater than about 1.5 M, broad and bimodal molecular weight distributions were observed. An extended homogeneous kinetic model that includes chain transfer to polymer predicted the polydispersities reasonably well. This model also predicted a region of inoperability that matched the experimental results. However, the extended homogeneous model could not account for the bimodal distributions.

Introduction

The polymer industry is a major user and emitter of volatile organic compounds (VOCs). Many of these compounds are toxic and cause harm to the environment. As a result of growing pressure from environmental groups and government regulations (e.g., the Montreal Protocol in 1987 and the Clean Air Act Amendments in 1990), there has been considerable effort devoted to finding alternate solvents and processes that are environmentally benign. DeSimone and others have shown that supercritical carbon dioxide ($scCO_2$) is a viable medium for a number of polymerizations.[1−8] In addition to being environmentally benign, carbon dioxide (CO_2) is inexpensive and widely available, and there is no chain transfer to solvent. Carbon dioxide can replace water in many polymerizations, eliminating the need for wastewater treatment and reducing the energy required to dry the polymer.

There is considerable demand for poly(vinylidene fluoride) (PVDF) and its copolymers because of their competitive costs, their excellent chemical, thermal and mechanical stability, and their extraordinary piezoelectric and pyroelectric properties.[9] Poly(vinylidene fluoride) is produced commercially by emulsion and suspension polymerizations, both of which generate large quantities of wastewater and require substantial quantities of energy to dry the polymer. Moreover, the emulsion technique, and perhaps the suspension technique, currently involve the use of surfactants that contain perfluorooctanyl sulfonates (PFOS) that are nonbiodegradable and accumulate in living organisms. Perfluorooctanyl sulfonates also have been identified as persistent organic pollutants, and production of these surfactants is being challenged. As a result, synthesis of PVDF in $scCO_2$ is of heightened interest.

Charpentier et al.[10] have described a continuous process for precipitation polymerization of vinyl monomers in $scCO_2$. This process has been used to polymerize vinylidene fluoride (VF_2), with diethylperoxydicarbonate (DEPDC) as the free radical initiator.[11] Diisopropylperoxydicarbonate (DIPPDC) is used in some emulsion and suspension processes for manufacturing PVDF. However, its synthesis is more complex than that of diethylperoxydicarbonate. The decomposition kinetics of these two initiators are essentially the same.[12]

Charpentier et al.[11] also studied the solubilities of VF2, PVDF, and the solution of DEPDC and Freon 113 that was fed to the CSTR in $scCO_2$. Both the initiator solution and the monomer were found to be completely soluble over the whole range of conditions used in this research. The polymer was essentially completely insoluble, consistent with the results of Lora et al.[13]

Kinetic studies[11] showed that the rate of polymerization (R_p) of VF_2 in $scCO_2$ was approximately first order with respect to monomer and approximately half order with respect to initiator. However, the data at low initiator concentrations and high VF_2 concentrations suggested the presence of an inhibitor. The nature of the inhibition was not clearly defined. The VF2 that was used did not contain an inhibitor. Moreover, chromatographic analyses of the VF2 and $scCO_2$ provided no evidence of a contaminant in either stream, including O_2 in the $scCO_2$. Despite this, the $scCO_2$ was passed through a copper oxide column to remove any O_2 that might have been present at undetectable levels. This

[†] North Carolina State University.
[‡] University of North Carolina-Chapel Hill.
[§] Current address: Department of Chemical and Biological Engineering, The University of Western Ontario, London, Ontario, Canada N6A 5B9.
* To whom correspondence should be addressed. J. M. DeSimone: e-mail desimone@unc.edu; phone (919) 962-2166; Fax (919) 962-5467. G. W. Roberts: e-mail groberts@eos.ncsu.edu; phone (919) 515-7328; Fax (919) 515-3465.

10.1021/ma0203602 CCC: $22.00
Published on Web 08/31/2002

$$I \xrightarrow{k_D} 2f\ R^\bullet \quad \text{(Initiator Decomposition)}$$

$$R^\bullet + M \xrightarrow{k_M} P_1^\bullet \quad \text{(Chain Initiation)}$$

$$P_n^\bullet + M \xrightarrow{k_P} P_{n+1}^\bullet \quad \text{(Propagation)}$$

$$P_n^\bullet + P_m^\bullet \xrightarrow{k_{tc}} P_{n+m} \quad \text{(Termination by Combination)}$$

$$P_n^\bullet + P_m^\bullet \xrightarrow{k_{td}} P_n + P_m \quad \text{(Termination by Disproportionation)}$$

$$P_n^\bullet + M \xrightarrow{k_Q} P_n + M^* \quad \text{(Inhibition)}$$

Figure 1. Kinetic scheme to model the rate of polymerization.[11] M* is an inactive radical.

led Charpentier et al.[11] to speculate that the observed inhibition effect might be associated with chain transfer to monomer, with the formation of an unreactive radical, as shown in the "inhibition" reaction in Figure 1.

Charpentier et al.[11] found that a homogeneous kinetic model, based on the reactions in Figure 1, predicted the measured polymerization rates reasonably well. Figure 1 shows two termination reactions: combination and disproportionation. The relative importance of these two reactions was not determined in the research of Charpentier et al.[11] Both reactions are shown in Figure 1 to facilitate later discussion.

In the previous work on the polymerization of VF2[10,11] in $scCO_2$, the average molecular weights and the molecular weight distribution (MWD) were not discussed in detail. Clearly, the polymer properties will impact the feasibility of manufacturing this polymer by precipitation polymerization in $scCO_2$. The objectives of the present research were to understand the effect of reaction conditions on the average molecular weights and the MWD of the product produced in $scCO_2$ and to extend the earlier treatment of polymerization rates[11] to a wider range of conditions.

Experimental Section

Materials. The initiator (DEPDC) synthesis has been described in detail elsewhere.[11,12,14] The final product of the synthesis was a solution of approximately 0.4 M DEPDC in Freon 113. Vinylidene fluoride was donated by Solvay Research, Belgium, and used without further purification. Carbon dioxide (SFE/SFC grade) was donated by Air Products & Chemicals, Inc., and was passed through columns containing 5 Å molecular sieves (Aldrich) and copper oxide (Aldrich) to remove excess water and oxygen, respectively. All other chemicals were obtained from the Aldrich Chemical Co. and used as received.

Polymerization Apparatus and Procedure. Figure 2 is a schematic diagram of the continuous polymerization system that was used in this research. This equipment and the associated experimental procedure were similar to that described elsewhere,[10,11] the only change being a more efficient polymer recovery system.

The main component of the system was a thermostated, 800 mL stainless steel autoclave with an internal diameter of 8 cm. A magnetically coupled impeller was used to mix the contents of the reactor. Previous measurements of the residence time distribution showed that this reactor behaves as an ideal continuous stirred tank reactor (CSTR),[12] in the absence of polymer.

Isco syringe pumps were used to feed VF_2, CO_2, and the solution of DEPDC in Freon 113 continuously into the CSTR. The outlet stream from the reactor, consisting of the polymer, unreacted VF_2 and DEPDC, and CO_2, was directed by a four-way ball valve into one of three filter housings containing 1 μm filters. The solid polymer was collected on the filters according to the following procedure: During startup of the reactor, before steady state was attained, polymer was collected in filter F2 until it was completely filled. Valves V1 and V2 then were switched, so that polymer was being collected

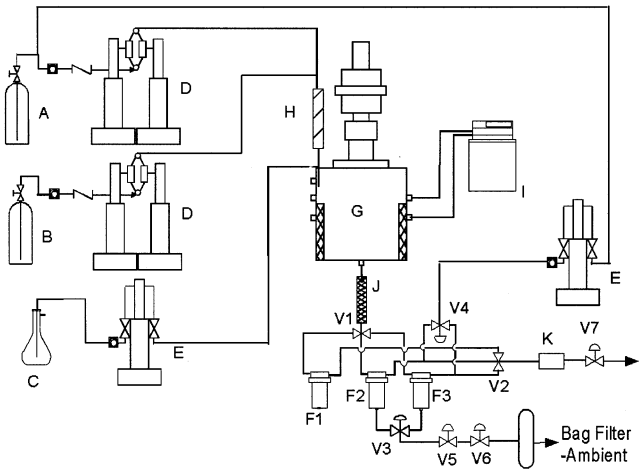

Figure 2. Continuous polymerization apparatus: A, CO_2 cylinder; B, monomer; C, initiator solution; D, continuous syringe pumps; E, syringe pumps; F1, steady-state filter; F2, F3, non-steady-state filter; G, thermostated autoclave; H, static mixer; I, chiller/heater unit; J, effluent cooler; K, gas chromatograph; V1, V2, four-way valves; V3, V4, three-way valves; V5, V6, two-way valves; V7, heated control valve.

in filter F3. Filter F2 was isolated, and polymer was discharged using a CO_2 flow through the filter in the reverse direction. Valves V5 and V6 then were actuated sequentially, with V5 being closed before V6 was opened, allowing the polymer to flow from the high-pressure filter housing into the bag filter, which was at ambient pressure. When filter F3 was full, the stream leaving the reactor was switched back to filter F2, and filter F3 was emptied using the same technique.

This procedure was repeated until the reactor had been operating at the desired conditions for five residence times and had reached steady state. The stream leaving the reactor then was switched to filter F1, which is referred to as the steady-state filter. Polymer was collected until F1 was filled with polymer. The system was then shut down, and the polymer in F1 was collected and weighed.

Analytical Techniques. The monomer conversion for a given polymerization experiment was determined gravimetrically by weighing the polymer collected in a defined period of time. The polymer was analyzed using gel permeation chromatography (GPC) and nuclear magnetic resonance spectroscopy (NMR). The GPC measurements were performed as described previously.[11] The NMR spectra were obtained on a Bruker 400 MHz (^{1}H) NMR spectrometer using XWIN-NMR software. The polymer was dissolved in DMF, and ^{19}F spectra were obtained using a 2.5 μs pulse with a 5 s delay. The NMR spectra were analyzed using the peak assignments reported by Russo et al.[15] after setting the main chain VF_2 peak, corresponding to normal head−tail addition of VF_2 units, to −91.6 ppm. The assignment for the end unit arising from addition of the first monomer to the initiator radical differed slightly from the reported value of 102.4 ppm because the initiator used in this research was different from that used by Russo et al.[15]

Results and Discussion

Molecular Weight Distribution (MWD) and Rate (R_p) Studies. Experiments were carried out to study the effect of inlet monomer concentration ($[M]_{in}$), average residence time in the reactor (τ), and temperature (T) on the rate of polymerization, R_p, the average molecular weights, and the MWDs. The results are summarized in Tables 1−3, and the MWDs are shown in Figures 3−5. In Tables 1−3, the initiator concentration in the stream leaving the reactor, $[I]_{out}$, was calculated from $[I]_{out} = \{[I]_{in}\}/\{(1 + k_D\tau)\}$. This relationship is based on the assumption that the experimental

Table 1. Effect of Inlet Monomer Concentration, $[M]_{in}$, on the Rate of Polymerization, R_p, and the Average Molecular Weights[a]

$[M]_{in}$ (mol/L)	$[M]_{out}$ (mol/L)	$[I]_{in}$ (mmol/L)	$[I]_{out}$ (mmol/L)	$R_p m$ (g/(min L))	$R_p/[M]_{out}[I]_{out}^{0.5}$ ($L^{0.5}$/($mol^{0.5}$ min))	$\bar{M}_n$ ($\times 10^{-3}$)	$\bar{M}_w$ ($\times 10^{-3}$)	PDI	$\bar{M}_n/R_p m$ (L min/g) ($\times 10^3$)
0.77	0.65	2.94	1.28	0.42	0.284	14.3	21.1	1.48	34.0
1.46	1.26	2.79	1.26	0.73	0.255	28.8	59.5	2.07	39.4
1.68	1.44	2.95	1.27	0.81	0.246	29.6	55.5	1.88	36.5
2.79	2.40	2.84	1.24	1.58	0.292	56.5	145	2.57	35.8
3.53	*b*	3.32	1.47	*b*	*b*	78.5	443	5.64	*b*

[a] $T = 75$ °C, $P = 27.7$ MPa (4000 psig), $\tau = 21$ min. [b] The data for R_p, $[M]_{out}$, and monomer conversion were not obtained for experiment 5 because of an error in recording the time during which steady-state polymer was collected.

Table 2. Effect of Temperature on the Rate of Polymerization, R_p, and the Average Molecular Weights; $P = 27.7$ MPa (4000 psig), $\tau = 11$ min

T (°C)	$[I]_{in}$ (mmol/L)	$[I]_{out}$ (mmol/L)	$[M]_{in}$ (mol/L)	$[M]_{out}$ (mol/L)	$R_p m$ (g/(min L))	$R_p/[M]_{out}[I]_{out}^{0.5}$ ($L^{0.5}$/($mol^{0.5}$ min))	$\bar{M}_n$ ($\times 10^{-3}$)	$\bar{M}_w$ ($\times 10^{-3}$)	PDI
85	2.56	0.82	2.62	0.65	2.00	0.464	32.2	57.5	1.8
75	2.79	1.26	1.46	1.26	1.48	0.226	42.6	103	2.4

reactor behaved as an ideal CSTR, in which $[I]_{out}$ is identical to the concentration of initiator in the reactor. Values of the decomposition rate constant, k_D, and the initiator efficiency, f, which are required in later calculations, were obtained from previous research.[12] The monomer concentration in the reactor and in the outlet stream, $[M]_{out}$, and R_p were calculated from the measured amount of polymer collected per unit time at steady state, again assuming an ideal CSTR.

Effect of Monomer Concentration. Five experiments were carried out with $[M]_{in}$ varying from 0.77 to 3.5 M at otherwise identical conditions. The results are given in Table 1 and Figure 3. To guide the interpretation of these data, consider a homogeneous polymerization involving only the first five reactions in Figure 1. The rate of polymerization, R_p (mol of monomer/(L min)), in an ideal CSTR at steady state is given by[16]

$$R_p = k_p[M]_{out}\lambda = \alpha[M]_{out}[I]_{out}^{0.5} \quad (1)$$

where

$$\lambda = \sum_{n=1}^{\infty} P_n^{\bullet} \quad (2)$$

$$\alpha = k_p(fk_D/k_t)^{0.5} \quad (3)$$

In eq 3, k_t is the termination rate constant, either k_{tc} or k_{td} or some combination thereof.

If termination is by disproportionation only, the number-average molecular weight, $\bar{M}_n$, is given by

$$\bar{M}_n = R_p m/2R_i \quad (4a)$$

where m is the molar mass of the monomer unit and R_i is the rate of initiation, $R_i = 2fk_D[I]_{out}$. The polydispersity index (PDI) ($= \{\bar{M}_w\}/\{\bar{M}_n\}$) is 2 if termination is by disproportionation only. If termination is by combination only,

$$\bar{M}_n = R_p m/R_i \quad (4b)$$

and the PDI is 1.5.

From Table 1, the ratio $R_p/[M]_{out}[I]_{out}^{0.5}$ is almost constant, consistent with eq 1. Moreover, R_i is constant for the first four experiments in Table 1, since $[I]_{out}$, f, and k_D are the same for each experiment. Therefore, the constancy of the ratio $\bar{M}_n/R_p$, as shown in the table, is consistent with eqs 4a and 4b. For these experiments,

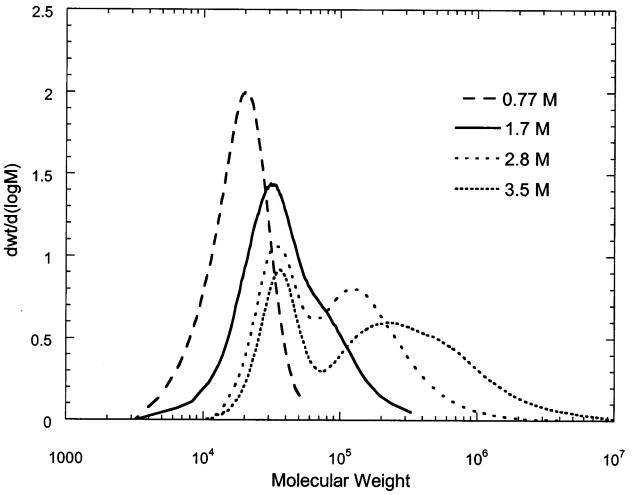

Figure 3. Effect of $[M]_{in}$ on MWD. $T = 75$ °C, $P = 27.7$ MPa (4000 psig). Other reaction conditions are presented in Table 1.

the simple homogeneous kinetic model embodied in eqs 1 and 4 provides a good description of the trends in R_p and $\bar{M}_n$.

The weight-average molecular weight, $\bar{M}_w$, increases with increasing $[M]_{in}$. However, the increase is not linear, as it would be if the PDI were constant. In fact, the PDI increases from 1.5 to 5.6 as the inlet monomer concentration increases from 0.77 to 3.5 M. Figure 3 shows that the MWD is unimodal with a PDI of around 1.5 at the lowest $[M]_{in}$. This suggests that termination is primarily by combination at these conditions. As $[M]_{in}$ increases, the MWD broadens and begins to exhibit a second mode. At the highest $[M]_{in}$ of 3.5 M, a bimodal MWD with a distinct high molecular weight peak is observed. Such behavior is not consistent with a homogeneous polymerization that proceeds according to the reactions in Figure 1.

Effect of Temperature. Two experiments were carried out at 75 and 85 °C. From Table 2, R_p at 85 °C was greater than that at 75 °C, despite the lower $[I]_{out}$ and $[M]_{out}$. Both $\bar{M}_n$ and $\bar{M}_w$ decreased with increasing temperature, as did the PDI. The MWD curves in Figure 4 show that the extent of bimodality decreased with increasing temperature.

Effect of Residence Time. Two sets of experiments, one at a low $[M]_{in}$ (0.78 M) and the other at a high $[M]_{in}$ (~2.8 M), were carried out to study the effect of average residence time, τ. Results are shown in Table 3. At $[M]_{in}$

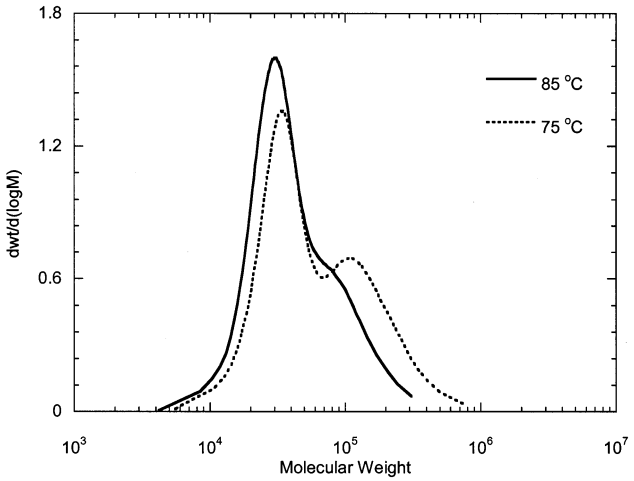

Figure 4. Effect of temperature on the MWD. $P = 27.7$ MPa (4000 psig), $\tau = 11$ min. Other reaction conditions are presented in Table 2.

$= 0.78$ M, R_p decreased with increasing τ. Since $[I]_{in}$ and $[M]_{in}$ were almost constant, both $[I]_{out}$ and $[M]_{out}$ decreased with increasing τ, thus resulting in a lower R_p. At $[M]_{in} = 0.78$ M, the ratio $\{R_p\}/\{[M]_{out}[I]_{out}^{0.5}\}$ was almost constant, consistent with eq 1.

Equation 4 predicts that the quantity $\bar{M}_n[I]_{out}/R_p$ should be constant as τ is varied. The data in Table 3 are reasonably consistent with this prediction. The number-average molecular weight is essentially independent of τ since R_p and R_i both decrease with increasing τ, resulting in a negligible combined effect on $\bar{M}_n$. The value of the PDI suggests that termination is by combination at the lower monomer concentration. Values of the PDI below 1.5 are impossible theoretically for a polymerization that takes place in an ideal CSTR according to the reactions of Figure 1. The PDI values in Tables 1 and 3 that are slightly below 1.5 probably resulted from small errors in measuring the tail of the MWD.

Figure 5 shows the effect of τ on the MWD. At the low $[M]_{in}$ (Figure 5A), the effect of τ on the MWD is negligible. The curves in Figure 5A are almost coincident and are perfectly unimodal. This behavior is typical of a homogeneous free radical polymerization in a CSTR, as the lifetime of a radical from initiation to termination is orders of magnitude smaller than the average residence time. Therefore, the average residence time has no effect on the average molecular weights and on the MWD at the lower monomer concentration.

In the second set of experiments, at the higher inlet monomer concentration, the values of $\{R_p\}/\{[M]_{out}[I]_{out}^{0.5}\}$ and $\bar{M}_n[I]_{out}/R_p$ are reasonably consistent with the simple homogeneous model. However, the PDI is about 2.5 for τ between about 11 and 20 min, and it increases sharply to 6.6 at $\tau = 25$ min. Figure 5B shows

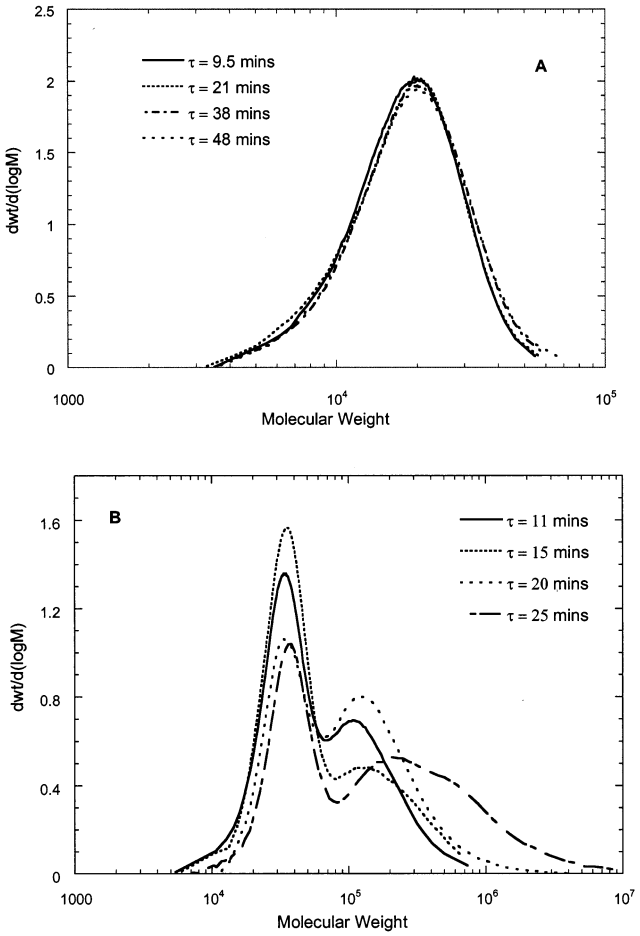

Figure 5. Effect of τ on the MWD: A, low $[M]_{in}$ (0.78 M); B, high $[M]_{in}$ (~2.8 M). $T = 75$ °C, $P = 27.7$ MPa (4000 psig). Other reaction conditions are presented in Table 3.

that the MWDs are bimodal at the higher monomer concentration. Moreover, at a residence time of 25 min, there is a significant shift in the second mode of the MWD to higher molecular weights. The behavior of $\bar{M}_w$ and the PDI is inconsistent with the simple homogeneous model.

Polymerization Rate Model. A homogeneous kinetic model that incorporated an inhibition step was developed previously by Charpentier et al.[11] to predict the polymerization rates. One version of this model was based on the reactions shown in Figure 1. For these reactions, the rate of polymerization, R_p, is given by[11]

$$\frac{R_p}{[M]_{out}} = \alpha([I]_{out}^{0.5} - \beta + \{\beta^2/2[I]_{out}^{0.5}\}) \qquad (5)$$

where α is given by eq 3, $\delta = (k_Q/4k_t)/(fk_D/k_t)^{0.5}$, and $\beta = \delta[M]_{out}$.

Table 3. Effect of Residence Time, τ, on the Rate of Polymerization, R_p, and the Average Molecular Weights; $T = 75$ °C, $P = 27.7$ MPa (4000 psig)

τ (min)	$[I]_{in}$ (mmol/L)	$[I]_{out}$ (mmol/L)	$[M]_{in}$ (mol/L)	$[M]_{out}$ (mol/L)	$R_p m$ (g/(min L))	$R_p/[M]_{out}[I]_{out}^{0.5}$ ($L^{0.5}$/($mol^{0.5}$ min))	$\bar{M}_n$ ($\times 10^{-3}$)	$\bar{M}_w$ ($\times 10^{-3}$)	PDI	$\bar{M}_n[I]_{out}/R_p m$ (L min/g)
9.6	2.89	1.83	0.78	0.70	0.58	0.300	14.7	20.4	1.39	46.4
21.5	2.94	1.28	0.78	0.65	0.42	0.286	14.3	21.1	1.48	43.6
38.3	2.93	0.89	0.78	0.61	0.31	0.267	15.2	21.5	1.41	43.6
48.3	2.94	0.75	0.78	0.58	0.28	0.270	15.3	22.1	1.44	41.0
11.2	2.67	1.59	2.75	2.55	1.48	0.228	42.6	103	2.42	45.8
15.0	2.63	1.38	2.85	2.65	1.11	0.176	41.5	100	2.41	51.6
20.5	2.84	1.27	2.79	2.40	1.58	0.288	56.5	145	2.57	45.4
25.5	2.86	1.13	2.90	2.44	1.52	0.290	67.0	441	6.58	49.8

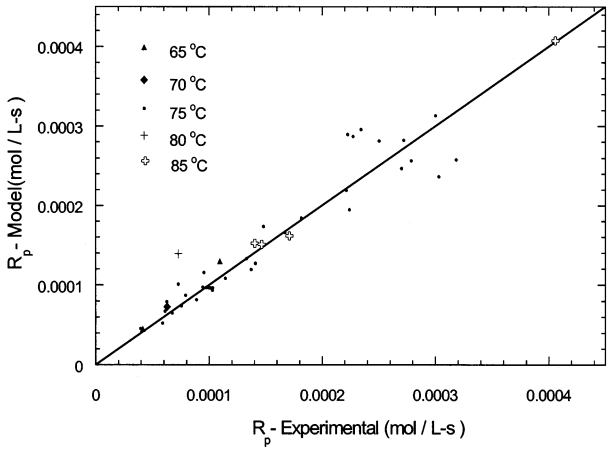

Figure 6. Parity plot showing fit of experimental data for R_p to that predicted by eq 5: $\alpha(75\ °C) = 4.76 \times 10^{-3}$ ($L^{0.5}/(mol^{0.5}\ s)$); $\delta(75\ °C) = 6.88 \times 10^{-3}$ $(L/mol)^{0.5}$; $E_a(\alpha) = 121.3$ kJ/mol; $E_a(\delta) = 60.8$ kJ/mol.

Figure 6 is a parity plot comparing the measured R_p to those predicted by eq 5. The experimental data consist of all the data reported earlier[11] plus that contained in Tables 1−3. The four kinetic parameters, α and δ at 75 °C, and their respective activation energies, $E_a(\alpha)$ and $E_a(\delta)$, were determined using nonlinear regression as described previously.[11] The resulting values were $\alpha(75\ °C) = 4.76 \times 10^{-3}(L^{0.5}/(mol^{0.5}\ s))$, $E_a(\alpha) = 121.3$ kJ/mol, $\delta(75\ °C) = 6.88 \times 10^{-3}$ $(L/mol)^{0.5}$, and $E_a(\delta) = 60.8$ kJ/mol. The values of $\alpha(75\ °C)$ and $\delta(75\ °C)$ are within 5% of those reported by Charpentier et al.[11] However, there are significant differences in the values of $E_a(\alpha)$ and $E_a(\delta)$. The present values should provide a more accurate description of the polymerization kinetics since this study includes much more data at temperatures other than 75 °C.

The monomer inhibition model predicts the rates reasonably well. Although the data scatter at the higher rates, the scatter is random. A model[14] that included only the first five reactions in Figure 1, and ignored the inhibition reaction, had about twice the sum of squared error as the monomer inhibition model. Moreover, deviations between the data and the predictions of the model without inhibition appeared to be systematic rather than random.

Bimodal Molecular Weights. A high PDI and bimodality of the MWD can contribute to improved flow characteristics and processing behavior.[17,18] Hence, a single step process for producing polymers with a bimodal MWD may be of significant interest. However, it is important to understand the source of the bimodal MWD and to be able to control the relative amounts and molecular weights of the two fractions. Since the reactions in Figure 1, occurring homogeneously, cannot account for the broad, bimodal MWDs observed in this study, several hypotheses have been explored in an attempt to explain this behavior. Two of these hypotheses, long chain branching and imperfect mixing, are discussed below.

Imperfect Mixing. Zhang et al.[19] have shown that imperfect mixing in a CSTR can lead to bimodal MWDs. In an earlier study of VF_2 polymerization in $scCO_2$, Charpentier et al.[11] demonstrated that the speed and type of agitation did not affect the average molecular weights and the R_p at low (0.77 M) inlet monomer concentration. The concentration of solids in the reactor in those experiments was around 10 g/L. However, the GPC data presented in Figures 3−5 show that broad and bimodal MWDs were obtained only at higher monomer concentrations. These factors caused us to reexamine the effect of mixing at higher $[M]_{in}$'s.

Table 4. Effect of Mixing on the Rate of Polymerization, R_p, and the Average Molecular Weights[a]

agitation speed (rpm)	type of agitator	$R_p m$ (g/(min L))	monomer conv, x (%)	$\bar{M}_w$ ($\times 10^{-3}$)	$\bar{M}_n$ ($\times 10^{-3}$)	PDI
1300	D	1.16	16.0	59.2	159	2.7
1800	D	1.26	17.4	52.0	145	2.8
2700	D	1.44	19.8	60.0	142	2.4
1800	UP	1.41	19.5	59.4	161	2.7
1800	D + DP[b]	1.62	22.4	62.1	146	2.4
1800	2 DP	1.47	20.3	62.1	159	2.6

[a] $T = 75$ °C; $P = 27.7$ MPa (4000 psig); $\tau = 20$ min; $[M]_{in} = 2.8$ M; $[I]_{in} = 2.8$ mM; $[I]_{out} = 1.27$ mM; D = dispersimax agitator (3.2 cm diameter), UP = upward pumping agitator (4 blades, 45° pitch, 5 cm diameter), DP = downward pumping agitator (three blades, 45° pitch, 5 cm diameter). [b] Downward pumping agitator at feed level.

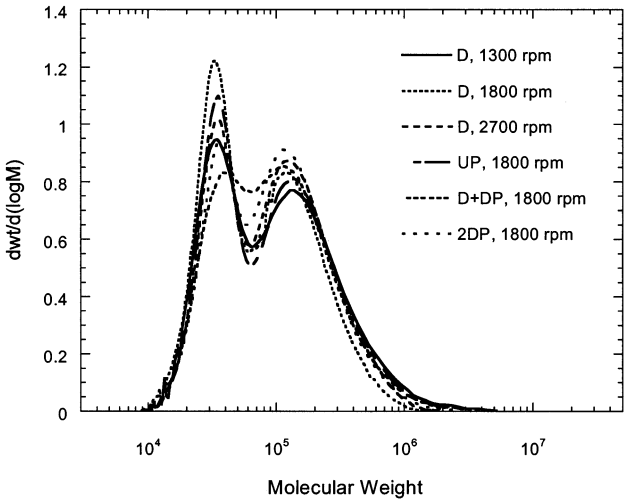

Figure 7. Effect of agitation on the MWD. $T = 75$ °C; $P = 27.7$ MPa (4000 psig); $\tau = 20$ min; $[M]_{in} = 2.8$ M; $[I]_{in} = 2.8$ mM; $[I]_{out} = 1.27$ mM; D = dispersimax agitator, DP = downward pumping agitator, UP = upward pumping agitator. Pictures of agitators are available in ref 14.

Table 4 presents the effect of agitation on the average molecular weights and the R_p at an $[M]_{in}$ of 2.8 M, for which the solids concentration in the reactor was about 35 g/L. The first three experiments in Table 4 were carried out using a 3.2 cm diameter dispersimax agitator, a six-bladed Rushton-type turbine, at rotational speeds from 1800 to 2700 rpm. The remaining experiments were performed at a rotational speed of 1800 rpm with different agitator designs, as given in Table 4. The corresponding MWD curves are presented in Figure 7.

With a single dispersimax agitator, both the monomer conversion and R_p increased as the rotational speed was increased. The upward pumping agitator appears to provide better mixing than the dispersimax agitator, at the same rotational speed. The highest conversion and R_p were obtained with the dispersimax agitator, plus a second, downward pumping agitator located at the point where initiator, monomer, and CO_2 were fed into the system. These observations are in contrast to those at low $[M]_{in}$.[11]

The difference in R_p at the best and worst mixing conditions (experiments 1 and 5, respectively, in Table 4) was 0.48 g/(min L). The difference in R_p that is

calculated from eq 3 by setting $\delta = 0$ (no inhibition) and $\delta = 6.88 \times 10^{-3}$ (L/mol)$^{0.5}$, the value obtained by fitting the R_p data to the inhibition model, was about 0.5 g/(min L). The agreement between these two numbers suggests that the inhibition in R_p at the high monomer concentrations may be the result of imperfect mixing at high monomer concentrations and not to a chemical reaction involving the monomer.

Although the average molecular weights and the PDIs vary somewhat with the mixing conditions, the differences are not significant. Additionally, the MWDs for the different agitation experiments, shown in Figure 7, are very similar and are all bimodal. This indicates that imperfect mixing does not cause the bimodal MWDs and high PDIs observed at high monomer concentrations.

In another attempt to understand the effect of mixing on this polymerization, the viscosity of the reactor contents was estimated, using correlations from the literature, for the conditions of Table 1 and Figure 3. These calculations suggest that the viscosity increased by a factor of about 2 between the experiments with the lowest (0.77 M) and highest (3.5 M) monomer concentrations. It seems very unlikely that this relatively small change in viscosity could have caused the dramatic changes in MWD and PDI that are shown in Table 1 and Figure 3.

Long Chain Branching. Polydispersities greater than 2 were obtained in most of the polymerization experiments. Such broad distributions cannot result from a homogeneous polymerization involving only the reactions in Figure 1. However, long chain branching can lead to broadening of the MWDs.[20] Long chain branching can occur in free radical polymerizations through chain transfer to polymer and/or through terminal double bond polymerization. It has been established that branching does occur via chain transfer to polymer in polymers containing VF2 units.[18] Terminal double bonds can be formed either by chain transfer to monomer or by termination via disproportionation. However, there is no evidence in the literature for chain transfer to vinylidene fluoride monomer or for termination of PVDF chains by disproportionation. The PDIs of around 1.5 that were obtained in this study at low monomer concentrations suggest that termination is by combination only.

Nuclear magnetic resonance studies were carried out to study the structure of PVDF synthesized in $scCO_2$. A typical NMR spectrum, presented in Figure 8, shows the presence of $-CF_2-CH_3$ end groups at -107.3 ppm. This indicates that some type of chain transfer reaction took place and supports the hypothesis that chain transfer to polymer may be an important reaction during the polymerization of VF_2 in $scCO_2$, leading to long chain branches and high PDIs. The absence of a signal corresponding to unsaturated chain ends suggests that there is no chain transfer to monomer or termination by disproportionation.

Modeling the Molecular Weights. The effect of long chain branching on the MWD in a CSTR was examined almost 50 years ago[20] for the case of termination by disproportionation. All of the work to date[20−23] has shown that chain transfer to polymer, coupled with termination by disproportionation, leads to PDIs exceeding 2 but not to bimodal MWDs. However, there does not appear to be any published research that defines whether chain transfer to polymer, coupled with termination by combination, can give rise to a bimodal MWD. A homogeneous kinetic model has been developed to explore this possibility. This model was based on the reactions in Figure 1, with the additional step of chain transfer to polymer.

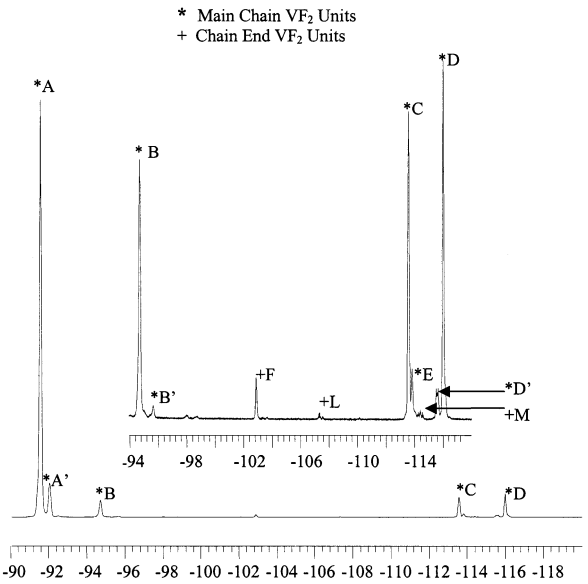

Figure 8. F-19 NMR spectrum of PVDF synthesized in $scCO_2$; the inset is a blowup of the region from -94 to -116 ppm. Peak assignments were obtained from Russo et al.[15]

$$P_n^{\bullet} + P_m \xrightarrow{mk_{tp}} P_m^{\bullet} + P_n \quad \text{(chain transfer to polymer)}$$

The inhibition step in Figure 1 was not included in the model because of the possibility that the observed deviation in R_p from first order with respect to monomer was due to imperfect mixing at high monomer concentrations rather than to an inhibition reaction. Moreover, termination by disproportionation was not considered.

Average Molecular Weights. The weight-average ($\bar{M}_w$) and number-average ($\bar{M}_n$) molecular weights were calculated for the above kinetic scheme in an ideal CSTR using the method of moments.[24,25] Briefly, the balance equations were written for the active radical species, $P_n^{\bullet}$, and the dead polymer species, P_n, for all n. Thus, two sets of equations, each comprising an infinite number of equations, were obtained. These sets were reduced to two equations using transforms. The average molecular weights were obtained from the zeroth (μ_0), first (μ_1), and second (μ_2) moments calculated from the transformed equations. The calculations are shown in detail elsewhere.[14]

Number-Average Molecular Weight. The number-average molecular weight calculated from the model is given by

$$\bar{M}_n = \mu_1 m/\tau k_{tc} \lambda^2 \tag{6}$$

where μ_1, the first moment of the dead polymer distribution, is given by

$$\mu_1 = [M]_{in} - [M]_{out} = R_p \tau \tag{7}$$

Equations 6 and 7 can be combined to give

$$\bar{M}_n = R_p m/k_{tc} \lambda^2 \tag{8}$$

The rate constant for chain transfer to polymer, k_{tp}, does not appear in eq 8, and R_p does not depend on k_{tp}.

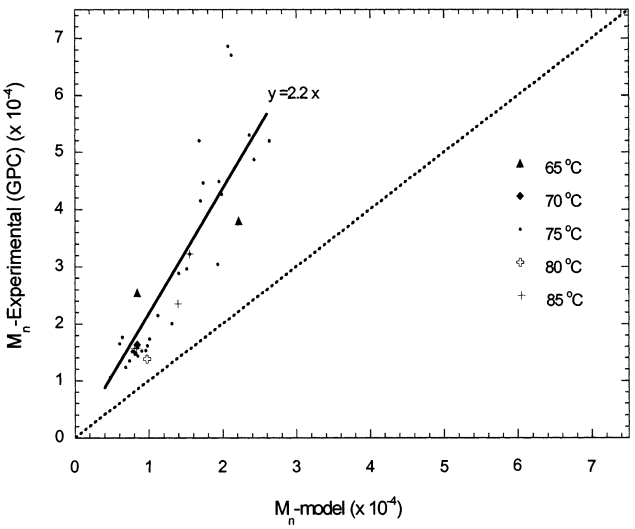

Figure 9. Parity plot showing fit of experimental (GPC) data to $\bar{M}_n$ predicted by eq 9.

Therefore, chain transfer to polymer has no effect on $\bar{M}_n$. Values of the number-average molecular weight were calculated from the measured rate of polymerization using

$$\bar{M}_n = R_p m(\text{measured})/k_{tc}\lambda^2 = R_p m(\text{measured})/fk_D[I]_{out} \quad (9)$$

Values of f and k_D were taken from a previous study of the decomposition of DEPDC in $scCO_2$,[12] and values of $[I]_{out}$ were calculated from $[I]_{in}$ using the same values of k_D, as discussed above.

Figure 9 is a parity plot of the $\bar{M}_n$ calculated from the GPC analysis vs the $\bar{M}_n$ predicted by eq 9. This plot contains 39 of the 44 data points in Figure 7; molecular weight data were not available for the other five points. All of the data points in Figure 9 fall well above the $y = x$ line, showing that the model (eq 9) substantially underpredicts the measured $\bar{M}_n$'s. The best fit, through the origin, of the data points has a slope of 2.2. Therefore, on average, the $\bar{M}_n$ measured by GPC is 2.2 times that predicted by the model.

The calculation of $\bar{M}_n$ relied on values of f and k_D that were measured in separate experiments.[12] The initiator concentration, $[I]_{out}$, was calculated from $[I]_{in}$, k_D, and τ. Therefore, any error in the value of $fk_D[I]_{out}$ could only be due to f and/or k_d. On the basis of previous studies, it appears that the value of k_D is accurate, since the measured values in $scCO_2$ compared very well to theory and to those measured in conventional solvents at atmospheric pressure.[12] However, the value of $f = 0.6$ that was used in these calculations may be too high. This value was measured in pure CO_2, in the absence of VF_2 and polymer, and represents the efficiency of the reaction between ethoxy radicals and galvinoxyl radicals.[12] The efficiency of the reaction between ethoxy radicals and VF_2 monomer in the presence of CO_2 and PVDF may not be the same. In fact, for a value of $f = 0.27$ ($0.6 \div 2.2$), there would be good agreement between the predicted and measured values of $\bar{M}_n$.

Weight-Average Molecular Weight. The weight-average molecular weight is given by

$$\bar{M}_w = \mu_2 m/\mu_1 \quad (10)$$

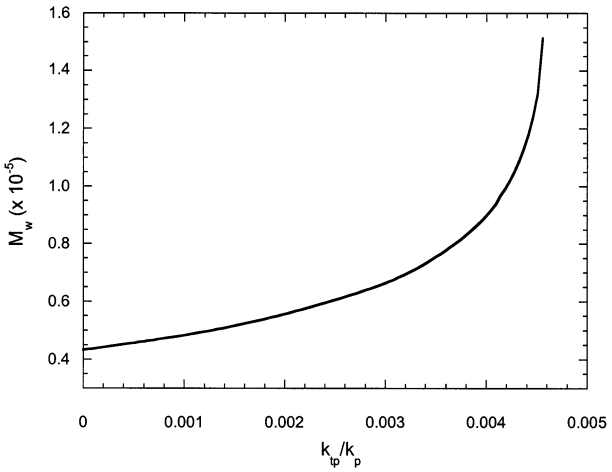

Figure 10. Effect of chain transfer to polymer on the weight-average molecular weight. $k_p/(k_{tc})^{0.5} = 0.19$ (L/(mol s))$^{0.5}$; $k_D = 0.00103$ s^{-1}; $f = 0.6$; $[M]_{in} = 3$ M, $[I]_{in} = 0.003$ M; $\tau = 20$ min; $T = 75$ °C.

If $k_{tp} \neq 0$, the second moment μ_2 is given by

$$\mu_2 = (-p_1 - \sqrt{p_1^2 - 4p_2})/2 \quad (11a)$$

where

$$p_1 = \frac{2a}{b} + \frac{[M]_{out}k_p}{bk_{tc}\lambda} - \frac{1}{2\tau k_{tc}b^2\lambda^2}$$

$$p_2 = \frac{a^2}{b^2} + \frac{[M]_{out}k_p a}{b^2 k_{tc}\lambda} + \frac{\mu_1}{2\tau k_{tc}b^2\lambda^2}$$

$$a = \frac{[M]_{out}k_p + 2k_{tc}\lambda}{\mu_1 k_{tp} + 2k_{tc}\lambda}$$

$$b = \frac{k_{tp}}{\mu_1 k_{tp} + 2k_{tc}\lambda}$$

If $k_{tp} = 0$,

$$\mu_2 = 2\tau\lambda a(k_{tc}a\lambda + [M]_{out}k_p) + \mu_1 \quad (11b)$$

The derivations of these equations are shown elsewhere.[14] Since μ_1 is independent of k_{tp}, the dependence of μ_2 on k_{tp} determines the dependence of $\bar{M}_n$ on k_{tp}.

Figure 10 is a plot of the effect of chain transfer to polymer on $\bar{M}_w$, calculated using eqs 10 and 11, for one particular set of experimental conditions. In these calculations, the ratio $(k_p/k_{tc})^{0.5}$ determined from the rate model (Figure 6) and the initiator efficiency, f, and the initiator decomposition rate constant, k_D, determined in previous research[12] were used. Figure 10 shows that $\bar{M}_w$ increases with increasing k_{tp}/k_p, with the rate of increase becoming very high at values above about 0.004. Beyond a "critical" value of k_{tp}/k_p, in this case about 0.0045, the calculated value of $\bar{M}_w$ becomes imaginary, as the expression under the square root in eq 11a becomes negative.

Polydispersity Index (PDI). From eqs 6 and 10, the PDI is given by $(\mu_2/\tau k_{tc}\lambda^2)$. Figure 11 shows the predicted and measured PDIs for the experiments in Table 1. A value of the ratio k_{tp}/k_p was calculated from the data point at an inlet monomer concentration of 3.5 M; the same value was used at the other concentrations. The

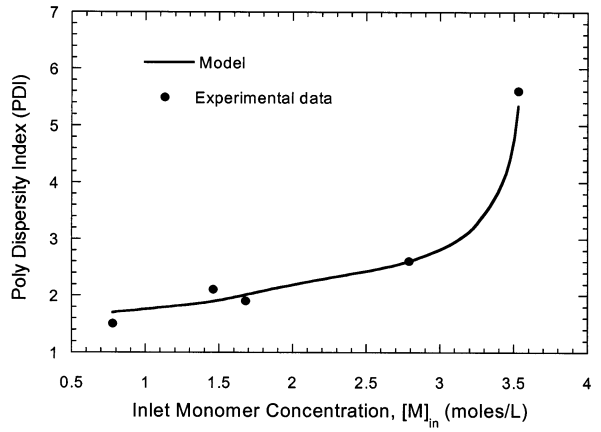

Figure 11. Effect of inlet monomer concentration on PDI. $k_D = 0.00103\ s^{-1}$; $f = 0.6$; $k_p/(k_{tc})^{0.5} = 0.19$ (L/(mol s))$^{0.5}$; $k_{tp}/k_p = 2.6027 \times 10^{-3}$. All other reaction conditions as presented in Table 1.

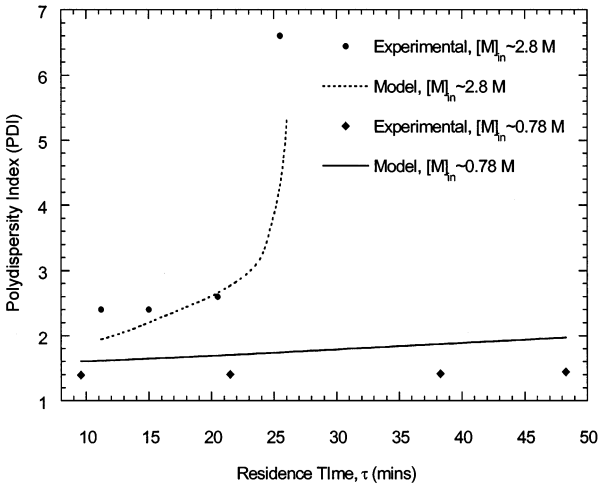

Figure 12. Effect of average residence time on PDI. $k_D = 0.00103\ s^{-1}$; $f = 0.6$; $k_p/(k_{tc})^{0.5} = 0.19$ (L/(mol s))$^{0.5}$; $k_{tp}/k_p = 2.6027 \times 10^{-3}$. All other reaction conditions as presented in Table 3.

calculated PDI is insensitive to the value of the initiator efficiency if $k_p/(k_t)^{0.5}$ is calculated from α for the corresponding value of f.[14]

Figure 12 shows the predicted and measured PDIs for the experiments in Table 3. The kinetic parameters shown in Figure 11 were used to calculate the predicted PDIs. Although the model could not reach a PDI of 6.6, as measured for the experiment at the longest residence time at the highest monomer concentration, Figure 12 does predict the abrupt increase in the measured PDI as τ is increased at $[M]_{in} = 2.8$ M. It also predicts that the PDI is insensitive to τ at low $[M]_{in}$.

Reactor Operability. The model predicts an imaginary value of $\bar{M}_w$ at certain conditions. For example, at $[M]_{in} = 2.8$ M, $\bar{M}_w$ is imaginary for τ greater than about 25 min. As τ is increased toward this point, the model predicts a steep increase in the value of $\bar{M}_w$. This behavior is similar to that seen at the onset of gelation, which refers to the formation of an infinite network in which polymer molecules have been cross-linked to form a macroscopic molecule.[16,24] This is associated with a drastic physical change in the polymer and a sharp increase in viscosity. In free radical polymerizations, gelation requires a linking reaction such as termination by combination[22,26] and cannot occur in the presence of chain transfer to polymer alone. The term "gel point" will be used to refer to the conditions at which the model predicts an imaginary value for $\bar{M}_w$.

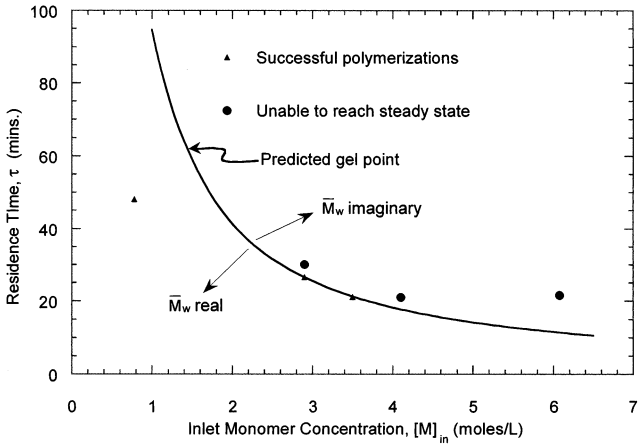

Figure 13. Predicted regions of operability and inoperability based on locus of gel points. The weight-average molecular weight is imaginary for all combinations of τ and $[M]_{in}$ above the solid line. The weight-average molecular weight is real and finite below the line. $T = 75$ °C; $P = 27.7$ MPa (4000 psig); $f = 0.60$; $[I]_{in} = 2.8$ mM; $k_D = 1.03 \times 10^{-3}\ s^{-1}$; $k_p/(k_{tc})^{0.5} = 0.19$ (L/(mol s))$^{0.5}$; $k_{tp}/k_p = 2.6027 \times 10^{-3}$.

The solid line in Figure 13 shows how the predicted location of the gel point depends on residence time and inlet monomer concentration, at otherwise constant conditions. Above the line, the model predicts an imaginary $\bar{M}_w$. Below the line, the predicted value of $\bar{M}_w$ is real and finite.

Experiments were attempted at three conditions that were above the predicted locus of gel points, as shown in Figure 13. None of these experiments reached steady state, as it became impossible to remove polymer continuously from the reactor. In fact, at $[M]_{in}$ of about 6 M and τ of about 20 min, the reactor filled with a hard, solid mass of polymer that was not soluble in any solvent. This supports the theory that gelation can occur at these conditions. However, the observed "gelation" in this case may involve agglomeration or vitrification of the polymer particles.

Figure 13 also shows three experiments that were carried out successfully close to, but nevertheless below, the predicted locus of gel points. These results provide a rather dramatic confirmation of the utility of the simple homogeneous kinetic model.

Complete MWD. The entire MWD is required to determine whether bimodality can result from chain transfer to polymer plus termination by combination. An analytical solution for the entire MWD could not be obtained because of the mathematical complexity arising from the presence of both chain transfer to polymer and termination by combination. However, a recursive algorithm to numerically calculate $P_n^\bullet$ and P_n from $P_{n-1}^\bullet$ and P_{n-1} was developed. This algorithm is presented elsewhere.[14] The values of P_n were used to construct a plot of n^2P_n vs n, which can be compared directly with the MWD curves determined by GPC.

Figure 14 shows the calculated MWD curves for two values of k_{tp}/k_p. The calculations were performed up to a chain length of 7000 monomer units, well beyond the values of n at which the peaks in the MWD curves were observed experimentally. The other parameters in Figure 14 were chosen to lie in the range where the GPC results showed bimodal distributions. Although the

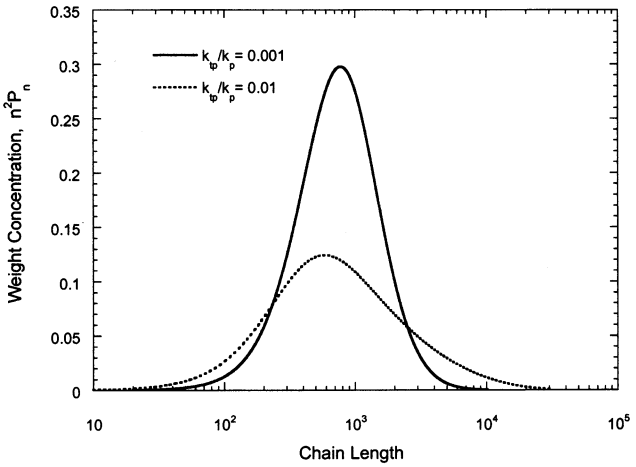

Figure 14. Effect of chain transfer to polymer on MWD. $k_D = 0.00103\ s^{-1}$; $f = 0.6$; $k_p/(k_{tc})^{0.5} = 0.19$ (L/(mol s))$^{0.5}$; $[M]_{in} = 3$ M; $[I]_{in} = 0.003$ M; $\tau = 20$ min; $T = 75$ °C.

MWD is broader at the higher value of k_{tp}/k_p, the distribution is perfectly unimodal in both cases. Calculations at higher monomer concentrations and chain transfer constants also gave perfectly unimodal distributions.

Work is underway to determine whether these bimodal distributions result from the heterogeneous nature of the polymerization in $scCO_2$, i.e., whether the two modes are associated with different loci of polymerization, the fluid phase, as assumed throughout this paper, and the polymer phase, which has been ignored in the present model.

Discussion of Homogeneous Model. Although the polymerization of VF2 in $scCO_2$ is heterogeneous, the utility of the simple homogeneous kinetic model presented herein is remarkable. This model contains four parameters: f, k_D, $(k_p/k_{tc})^{0.5}$, and (k_{tm}/k_p). The first two, f and k_D, were obtained from independent experiments.[12] The value of $(k_p/k_{tc})^{0.5}$ was calculated from the value of α that resulted from fitting the R_p data, as discussed above. The final parameter (k_{tm}/k_p) was obtained by fitting the PDI of a single experiment. Nevertheless, the simple homogeneous model is able to predict R_p, PDI, and the region of reactor operability reasonably well. The latter capability is particularly impressive and important. Moreover, the model would provide accurate predictions of the average molecular weights, with no loss in other predictive capabilities, if the initiator efficiency, f, were adjusted downward.

The ability of the homogeneous model to describe the behavior of this complex polymerization may be fortuitous, or it may be that polymerization of VF2 in $scCO_2$ is predominantly homogeneous. For example, the kinetics of polymerization may be much faster than the kinetics of polymer precipitation. The lifetime of a polymer radical from initiation to termination is of the order of milliseconds. If precipitation is much slower, most polymer chains will grow and terminate in the fluid phase. Although a heterogeneous model ultimately may be required to explain the bimodal MWD, such a model inevitably will involve many more adjustable parameters.

Conclusions

Polymerizations of VF_2 in $scCO_2$ were carried out in a CSTR to study the effect of reaction conditions such as temperature, inlet monomer concentration, and residence time on the rate of polymerization and on the molecular weight distribution. A homogeneous kinetic model that incorporates inhibition by the monomer predicted the polymerization rates reasonably well. However, in mixing studies that were carried out at a high monomer concentration, the polymerization rate increased with increasing agitator speed and depended on agitator configuration to some extent. The inhibition observed in the polymerization rates may be related to small changes in mixing associated with increasing viscosity at higher monomer concentrations.

The MWD of the polymer was unimodal at lower inlet monomer concentrations (ca. 0.77−1.5 M), and the PDI was about 1.5. However, the MWD broadened, and a second mode appeared as the inlet monomer concentration was increased. Very high PDI values (>5) were obtained in experiments carried out at long residence times (<20 min) and high inlet monomer concentrations (<2.8 M). Nuclear magnetic resonance (NMR) results suggested that chain transfer to polymer may be a source of these high PDIs.

Two different possibilities, imperfect mixing and long chain branching, were explored in an attempt to explain the broad, bimodal MWDs. Mixing studies showed that the type and speed of agitation did not have significant effect on the average molecular weights and the shape of the MWD. A model that incorporated chain transfer to polymer and termination by combination was developed to study the effect of long chain branching on the MWD. This model predicted the variation of the PDI with residence time and inlet monomer concentration reasonably well. The model also successfully predicted a region in which the reactor could not be operated at steady state. However, the MWD curves predicted using the model were unimodal. Chain transfer to polymer can account for the breadth of the MWD but not for its bimodality.

Acknowledgment. This work was supported in part by Solvay Advanced Polymers, Inc., through the Kenan Center for the Utilization of Carbon Dioxide in Manufacturing. This work made use of STC shared experimental facilities supported by the National Science Foundation under Agreement CHE-9876674. We thank Solvay Research, Belgium, for performing the GPC analysis of the PVDF samples. Special thanks is extended to Dr. Roland Martin of Solvay for many helpful discussions.

References and Notes

(1) Canelas, D. A.; DeSimone, J. M. *Adv. Polym. Sci.* **1997**, *133*, 103−140.
(2) DeSimone, J. M.; Guan, Z.; Elsbernd, C. S. *Science* **1992**, *257*, 945−947.
(3) DeSimone, J. M.; Maury, E. E.; Menceloglu, Y. Z.; McClain, J. B.; Romack, T. J.; Combes, J. F. *Science* **1994**, *265*, 356−359.
(4) Kendall, J. L.; Canelas, D. A.; Young, J. L.; DeSimone, J. M. *Chem. Rev.* **1999**, *543*, 3−563.
(5) Sumitomo Chemical Company, French Patent 1524533, 1968.
(6) Hagiwara, M.; Mitsui, H.; Machi, S.; Kagiya, T. *J. Polym. Sci., Part A-1* **1968**, *6*, 603−608.
(7) Sertage, W. G., Jr.; Davis, P.; Schenck, H. U.; Denzinger, W.; Hartmann, H. Canadian Patent 1274942, 1968.
(8) Herbert, M. W.; Huvard, G. S. European Patent Application 88112198.2, 1988.
(9) Lovinger, A. J. In *Development in Crystalline Polymers-1*; Bassett, D. C., Ed.; Applied Science Publishers: London, 1982; pp 195−273.
(10) Charpentier, P. A.; Kennedy, K. A.; DeSimone, J. M.; Roberts, G. W. *Macromolecules* **1999**, *32*, 5972−5975.

(11) Charpentier, P. A.; DeSimone, J. M.; Roberts, G. W. *Ind. Eng. Chem. Res.* **2000**, *39*, 4588−4596.
(12) Charpentier, P. A.; DeSimone, J. M.; Roberts, G. W. *Chem. Eng. Sci.* **2000**, *55*, 5341−5349.
(13) Lora, M.; Lim, J. S.; McHugh, M. A. *J. Phys. Chem. B* **1999**, *103*, 2818−2822.
(14) Saraf, M. K. Polymerization of Vinylidene Fluoride in Supercritical Carbon Dioxide: Molecular Weight Distribution. M.S. Thesis, North Carolina State University, 2001.
(15) Russo, S.; Behari, K.; Chengji, S.; Pianca, M.; Barchiesi, E.; Moggi, G. *Polymer* **1993**, *34*, 4777−4781.
(16) Odian, G. *Principles of Polymerization*, 3rd ed.; John Wiley & Sons: New York, 1991.
(17) Tervoort, T.; Visjager, J.; Graf, B.; Smith, P. *Macromolecules* **2000**, *33*, 6460−6465.
(18) Maccone, J.; Apostolo, M.; Ajroldi, G. *Macromolecules* **2000**, *33*, 1656−1663.
(19) Zhang, S. X.; Ray, W. H. *AIChE J.* **1997**, *43*, 1265−1277.
(20) Beasley, J. K. *J. Am. Chem. Soc.* **1953**, *75*, 6123−6127.
(21) Crowley, T. J.; Choi, K. Y. *Ind. Eng. Chem. Res.* **1997**, *36*, 1419−1423.
(22) Mullikin, R. V.; Mortimer, G. A. *J. Macromol. Sci., Chem.* **1970**, *A4*, 1495−1505.
(23) Bamford, C. H.; Tompa, H. *Trans. Faraday Soc.* **1954**, *50*, 1097−1115.
(24) Dotson, N. A.; Galvan, R.; Laurence, R. L.; Tirrell, M. *Polymerization Process Modeling*; VCH Publishers Inc.: Weinheim, 1996.
(25) Graessley, W. W.; Mittelhauser, H.; Maramba, R. *Makromol. Chem.* **1965**, *86*, 129−138.
(26) Tobita, H. *J. Polym. Sci., Part B: Polym. Phys.* **1993**, *31*, 1363−1371.

MA0203602